Advances in Industrial and Manufacturing Engineering 10 (2025) 100157

Contents lists available at ScienceDirect

Advances in Industrial and Manufacturing Engineering

journal homepage: www.sciencedirect.com/journal/advances-in-industrial-and-manufacturing-engineering

Manufacturing of irregular shapes through force control in incremental sheet forming with active medium

Sebastian Thiery [a,*], Mazhar Zein El Abdine [a], Jens Heger [a], Noomane Ben Khalifa [a,b]

[a] Institute for Production Technology and Systems, Leuphana University Lüneburg, Universitätsallee 1, 21335, Lüneburg, Germany
[b] Institute of Material and Process Design, Helmholtz-Zentrum Hereon, Max-Planck-Str. 1, 21502, Geesthacht, Germany

ARTICLE INFO

Keywords:
Incremental sheet forming
Active medium
Irregular shape
Forming forces
Geometrical accuracy

ABSTRACT

Convex shapes can be created in incremental sheet forming by supporting the workpiece with the pressure of an active medium. In this paper, a method is presented for creating irregular convex shapes by adjusting the pressure to control the forming forces. At first, the general characteristics of the forming forces in incremental sheet forming with active medium (IFAM) are investigated based on a truncated pyramid and a truncated cone. The findings show that the pressure has to be adapted for each contour of the toolpath to achieve a specific wall angle. However, this strategy cannot be applied for an irregular shape consisting of half a truncated pyramid and half a truncated cone since the forming forces fluctuate over one contour. To enhance the control approach, a data set is subsequently generated by recording the forming forces under the influence of the wall angle. The data analysis reveals a strong correlation between the height difference per contour and the tangential force. Finally, a control concept is proposed to adjust the tangential force and is subsequently validated on the irregular-shaped part. The results prove that irregular shapes require a sophisticated control of the forming forces to increase the geometrical accuracy.

1. Introduction

Incremental sheet forming processes are flexible and offer the advantage of quickly manufacturing a desired product based on its CAD drawing. Current research trends share the common goal of creating irregular and complex parts with customized freeform surfaces, for example as medical applications or industrial components (Duflou et al., 2018). Process parameters, including the geometry of the workpiece correlate with the forming forces during manufacturing, which is why investigations of the underlying mechanisms are necessary. In addition, closed-loop control and process monitoring provide new possibilities to improve the manufacturing process.

Simple shapes created by incremental sheet forming can have a single concave or convex feature. When the workpiece is not supported on the tool-averted side while simultaneously being shaped by one tool, the process is referred to as single-point incremental forming (SPIF). However, complex shapes can be a combination of concave and convex features, which are hardly producible without supporting the workpiece. One way to produce combined convex-concave components is two-point incremental forming (TPIF) by using a solid die under the workpiece. Taleb Araghi et al. (2011) used a solid die for an initial stretch forming step to create a convex shape followed by incremental forming to add concave pockets. This strategy offers the benefits of reduced forming time, less springback and improved sheet thinning. Another way is to use a second movable tool, which is defined as double-sided incremental forming (DSIF). Ndip-Agbor et al. (2018) developed an approach to automatically generate the toolpath for complex parts with multiple features in DSIF. Incremental forming with active medium (IFAM) is another way to create combined convex-concave components using pressure to support the workpiece from the bottom (Ben Khalifa and Thiery, 2019). Since the pressure has a significant effect on the geometry, Thiery et al. (2021) proposed a control approach based on an artificial neural network to adjust the pressure for each contour of the toolpath to increase the geometrical accuracy of a convex truncated cone. However, the shapes of industrial parts are often irregular as demonstrated on the example of a car fender by Bambach et al. (2009) using multi-stage SPIF. Irregular shapes are characterized by the fact that the wall angle and the step size can vary along one contour of the toolpath. Based on an ellipsoidal geometry, Li et al. (2015) showed that the tangential force in SPIF does not remain constant during one contour but changes locally as a result of the wall angle. In this regard, the correlation between force and geometry might

* Corresponding author.
E-mail address: sebastian.thiery@leuphana.de (S. Thiery).

https://doi.org/10.1016/j.aime.2025.100157
Received 1 October 2024; Received in revised form 17 December 2024; Accepted 10 February 2025
Available online 11 February 2025

be the key to enhancing the process control in IFAM.

In contrast to conventional sheet forming operations such as deep drawing, the forming forces in incremental sheet forming do not increase with the size of the workpiece because the contact zone and the step size are small (Jeswiet et al., 2005b). Different methods can be used to determine or to predict the forming forces in SPIF. Duflou et al. (2007) showed the effect of the step size between consecutive contours, the diameter of the tool, the wall angle and the thickness of the sheet metal on the forming force by measuring the forces experimentally with a table type dynamometer, which is connected with the fixture holding the workpiece. Furthermore, the forces could also be measured directly at the tool (Jeswiet et al., 2005a) or a sensor could be integrated into the tool holder (Thiery et al., 2021). Since the set-ups used for incremental sheet forming have a load limit regarding the axial and horizontal forces, it is necessary to estimate the forces beforehand or to measure them during the manufacturing process. Henrard et al. (2011) investigated the prediction of forming forces by finite element simulation showing that the type of element, the constitutive law and the identification of material parameters affect the result. To minimize the computational costs, the numerical model of a truncated cone can be reduced to a smaller section similar to a slice of a pie (Henrard et al., 2011). In contrast, analytical models require less computational resources than finite element simulation (Bansal et al., 2017). Bansal et al. (2017) developed an analytical approach to calculate the forming forces based on the shape of contact zone and the stresses within it and compared the results to different regression functions provided in the literature. Aerens et al. (2010) performed experiments to identify the influence of the process parameters similar to Duflou et al. (2007) and derived regression functions to calculate the forming forces. By including the tensile strength into equations, the regression functions can be generalized and applied for different materials (Aerens et al., 2010). Moreover, Liu and Li (2020) engaged an artificial neural network for predicting the forming forces. By using a virtual data generation approach, models can successfully be trained even in the case of insufficient experimental data during an early stage of SPIF implementation (Liu and Li, 2020).

Three different force components have to be considered in incremental sheet forming (Aerens et al., 2009). The *vertical force* is directed in the axial direction of the tool, the *tangential force* is parallel to the tool movement and the *radial force* is perpendicular to the tool movement. In SPIF, the forces start at zero in the first contour of the toolpath and quickly increase during the next contours until reaching a steady state (Duflou et al., 2007). When the tool moves from one contour to the next, there can be a short increase or decrease of the vertical force (Duflou et al., 2007). If the desired geometry has corners, for example a truncated pyramid, a short peak in all force components occur at these areas since the contact zone and the stress state change (Zhu and Ou, 2023). In particular, the tangential force can be affected by the wall angle and the vertical step size. Aerens et al. (2010) created parts with different wall angles while keeping the step size constant and using a rotating tool. Under these conditions, a trend in the tangential force could not be observed (Aerens et al., 2010). However, Li et al. (2014) performed comparable experiments with no tool rotation and showed an increase in the tangential force for increasing wall angles. Both studies noticed an increase of the tangential force for larger step sizes. The tangential force in incremental sheet forming can be furthermore used as an indicator for sheet failures such as ruptures (Fiorentino, 2013). Filice et al. (2006) demonstrated a monitoring system to detect imminent ruptures based on the trend of the tangential force and to automatically adapt the tool radius as well as the step size. In general, different types of closed-loop controls can be applied for metal forming processes (Allwood et al., 2016). Possible applications include an online control of the product geometry in SPIF (Allwood et al., 2009) or an online control of the forces in DSIF (Ren et al., 2018).

Closed-loop control is a possibility to adjust the pressure and to increase the geometrical accuracy of regular shapes in IFAM (Thiery et al., 2021). However, the manufacturing of irregular shapes requires deeper understanding of the forming forces during the manufacturing process and an adaptation of the control concept. Hence, in this manuscript, the characteristics of the forming forces in IFAM are first analyzed on the example of a truncated pyramid and a truncated cone. Subsequently, a data set is generated to identify the correlation between the wall angle and the tangential forming force. The full dataset is published and can be used to further develop and expand upon this research. Finally, a control concept is developed and tested for manufacturing an irregular convex part being half a truncated pyramid and half a truncated cone. To prove the feasibility, the geometrical accuracy of the novel force control is compared with the aforementioned method of controlling the part height.

2. Description of IFAM

2.1. Principle of the process

The procedure of IFAM is shown in Fig. 1. At first, the blank is fixed by the blankholder on top of a pressure chamber, creating a sealed space inside. The component can then be formed using both concave forming operations such as SPIF and media-assisted convex forming operations. The toolpath of a concave forming operation is three-dimensional and follows the target geometry, moving inward with each contour. In contrast, the tool moves in a horizontal plane from the center to the edge of the workpiece during a convex forming operation, resulting in a two-dimensional toolpath. By combining both forming operations, the manufacturing of combined convex-concave components is possible without having to turn the workpiece in the process (Ben Khalifa and Thiery, 2019). Unlike TPIF or DSIF, there is no need for a dedicated die or second moving tool. Another advantage is that the process can be carried out on a conventional milling machine. However, the two-dimensional toolpath of the convex forming operation does not contain the geometrical information of the target geometry in the vertical direction. Therefore, IFAM requires additional strategies to control the pressure and monitor the process.

Plastic yielding in IFAM results from the interaction between the tool and the pressure of the active medium. The Medium can be gaseous or liquid (Ben Khalifa and Thiery, 2019). In particular, the pressure is much lower than in hydroforming processes, so that it does not directly cause plastic deformation. Therefore, the material outside the contact area between tool and workpiece does not undergo plastic deformation. As sheet thinning is limited to the area formed by the tool, it can be calculated using the sine law, similar to other ISF processes (Thiery, 2023).

2.2. Control for regular shapes

The geometrical accuracy in IFAM is lower than the geometrical accuracy in DSIF (Ben Khalifa and Thiery, 2019). To improve the manufacturing process in this regard, different strategies have been developed including a two-stage forming method, conical tools and closed-loop control (Thiery, 2023). The control approach was designed with a discrete principle assuming that the upwards bulging of the material is homogenous along the circumferential of a truncated cone. Thus, it was sufficient to measure the part geometry after each contour of the toolpath and to adjust the pressure afterwards according to Fig. 2 (Thiery et al., 2021). However, the forming behavior of irregular components can change locally and the pressure has to be adapted within a contour. Since a continuous detection of the part height would require a slow feed rate or multiple stops of the tool movement to ensure an accurate measurement, the height cannot be used as a control variable for manufacturing irregular shapes. To that end, the aim of this work is to relate the target geometry to the forming force and subsequently use the forming force as a substitute for the control variable.

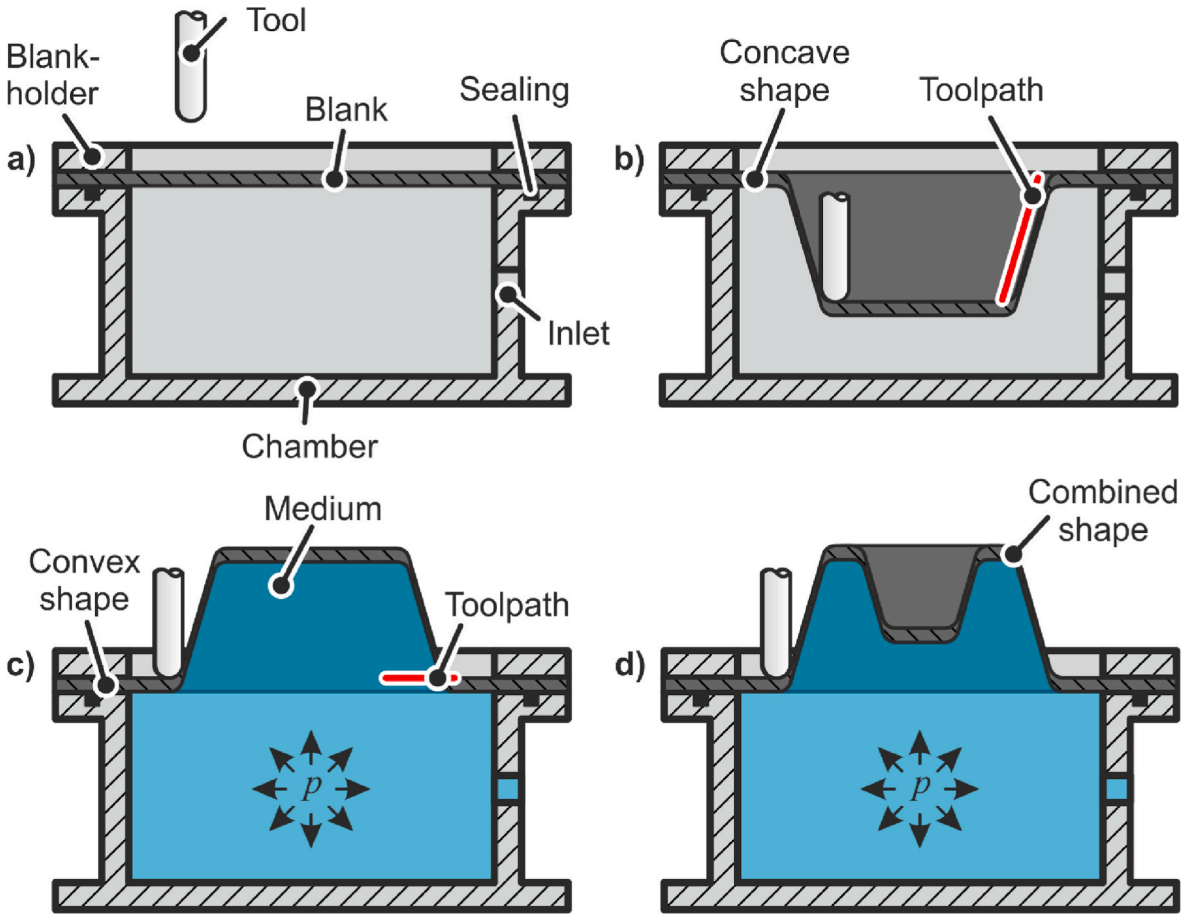

Fig. 1. Procedure of incremental sheet forming with active medium showing (a) the initial state, (b) an unsupported concave forming operation, (c) a convex forming operation supported by pressure and (d) the production of a combined component.

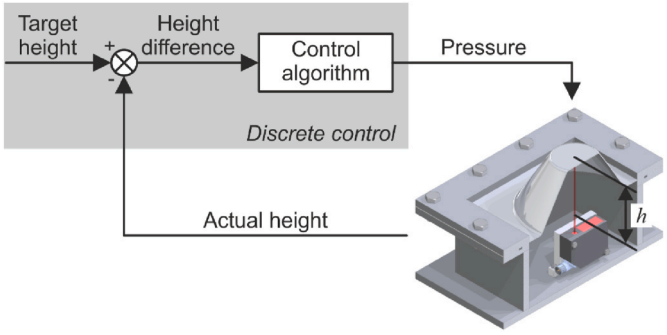

Fig. 2. Principle of the closed-loop control using an artificial neural network according to Thiery et al. (2021).

3. Characteristics of forming forces

3.1. Experimental set-up

The central component of the equipment needed for this process is a pressure chamber containing pressurized air, Fig. 3. The pressure is regulated by an external control valve in relation to the atmosphere ranging from 0.0 bar to 6.0 bar and monitored by both a manometer and a pressure sensor. When the pressure is released from the chamber, the same set-up can also be used for SPIF. The chamber is mounted on a force measuring platform from AMTI type MC12-4k and includes a laser distance sensor, which allows the detection of the part height during the forming process to a maximum of 100 mm. A computer is used to record the corresponding sensor signals and to implement a controller for adjusting the pressure level. The tool is attached to the spindle of the milling machine and has a hemispherical tip with a radius of 5 mm. Forming oil is used to reduce tool wear.

The two-dimensional toolpath progresses outwards while the convex profile of the product geometry, as shown in Fig. 4, emerges upwards with each contour of the toolpath. To study the characteristics of the forming forces and the relation with the geometrical accuracy, the manufacturing processes for a truncated pyramid, a truncated cone and a workpiece as combination of both are analyzed. The toolpaths consist of 40 contours with a horizontal step size of $\Delta x = 0.75$ mm, Fig. 2. The feed rate of the tool is set to $f = 1000$ mm/min and the rotational speed of the spindle is $n = 60$ rpm. Regarding the truncated pyramid, the width of the first contour and of the last contour are $d_0 = 90$ mm and $d_{40} = 148.5$ mm, respectively. Identical dimensions are selected for the truncated cone and the combined workpiece. The toolpath does not include information of the product in vertical direction. The tip of the tool moves to the top surface of the blank at the beginning and does not change during the process. However, the part height is observed using the laser distance sensor and controlled by adjusting the pressure to create a wall angle of $\alpha = 50°$, equivalent to a total height of 35.75 mm. The sheet material is AA1050A-H24 with $s = 1$ mm and the dimension 190 mm × 190 mm inside the clamping.

3.2. Pressure adjustment

The pressure during the manufacturing process is adjusted by a closed-loop control. Since the model-based control approach used by Thiery et al. (2021) was trained exclusively for truncated cones, a

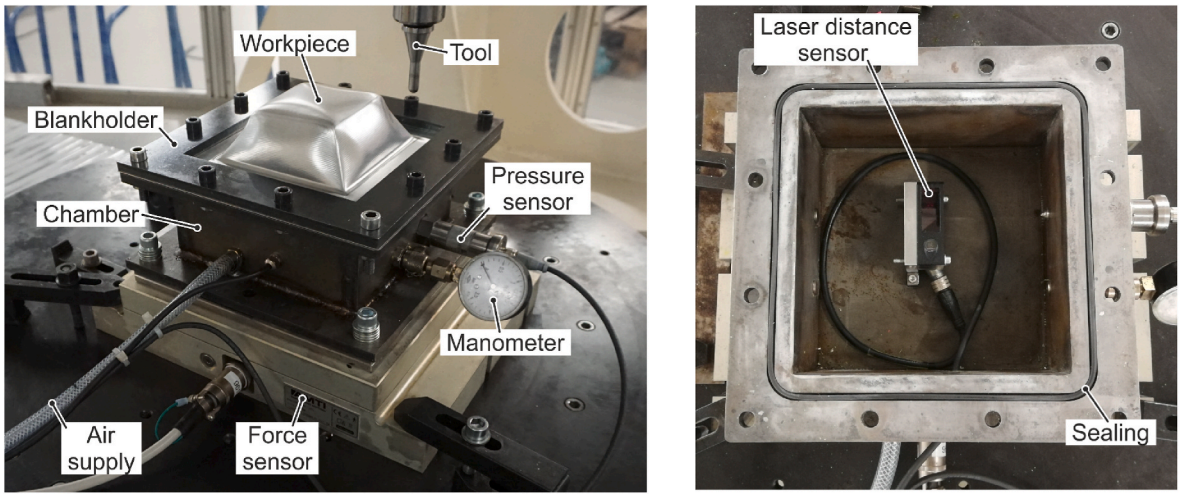

Fig. 3. Experimental set-up for incremental sheet forming with active medium.

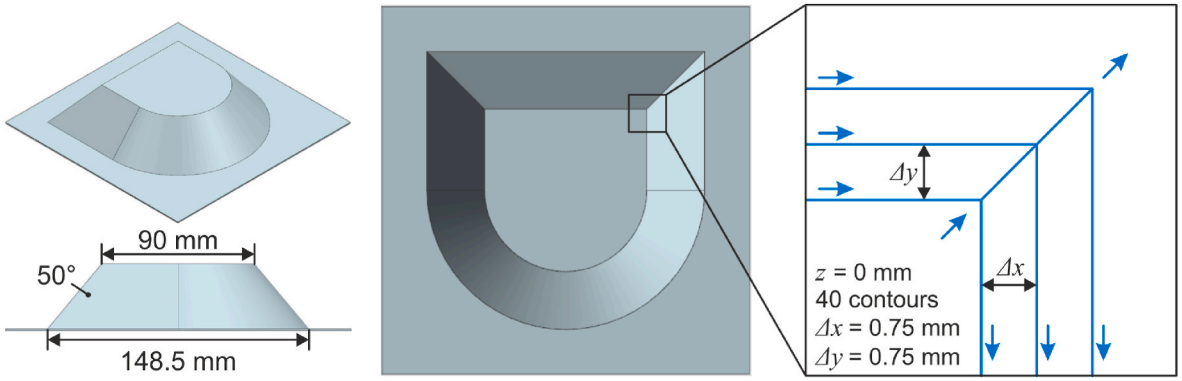

Fig. 4. Three-dimensional target geometry and two-dimensional toolpath for creating a convex irregular-shaped part.

geometry-independent controller with integral behavior is selected for this work. The computer, which is used to record the part height and to set the pressure, has a connection with the control of the milling machine for synchronization. The contours of the toolpath are numbered with i. After each contour, the part height is detected and used to calculate the difference $\Delta h_a(i)$ between the actual height $h_a(i)$ and the height at the beginning of the contour $h_a(i\text{-}1)$, Eq. (1).

$$\Delta h_a(i) = h_a(i) - h_a(i-1) \tag{1}$$

The target height difference $\Delta h_t(i)$ can be calulcated by the step size Δx and the wall angle α, Eq. (2)

$$\Delta h_t(i) = \tan\alpha \bullet \Delta x \tag{2}$$

The actual height difference $\Delta h_a(i)$ has to match its target value $\Delta h_t(i)$, which corresponds to the desired wall angle. The control error is used to increase or decrease the pressure level for the next contour, Eq. (3). The pressure level of the first contour and the control parameter are set to $p(1) = 0.4$ bar and $k = 0.05$ bar/mm, respectively. This closed-loop control, see Fig. 5, is implemented in the measurement and control software, which is running on the computer of the experimental set-up. The same software is modified during this work to integrate the force control.

$$p(i+1) = p(i) + [\Delta h_t(i) - \Delta h_a(i)] \bullet k \tag{3}$$

3.3. Calculation of the forming forces

The vertical forming force F_z and the horizontal forming forces F_x and F_y are recorded with a frequency of 50 Hz. Fig. 6 a) shows the continuous measurement signal during the 20th contour of the convex truncated pyramid. When the tool moves along the corner of the toolpath, a decrease of the vertical forming force F_z and a decrease or direction change of the forces F_x and F_y can be observed. In contrast, the forming forces in SPIF are related with an increase at the corner of the toolpath (Zhu and Ou, 2023). The direction of the forces F_x and F_y is defined by the orientation of the force measurement platform. However, the tangential force parallel to the tool F_t movement and the radial force perpendicular to the tool movement F_r have to be calculated, Fig. 6 b). With a linear tool movement, F_t and F_r correspond to the absolute values

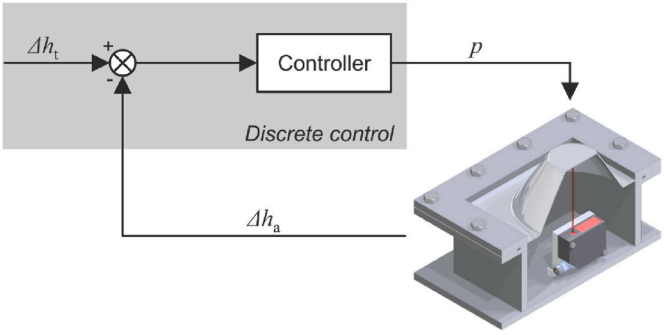

Fig. 5. Principle of controlling the height difference using a controller with integral behavior.

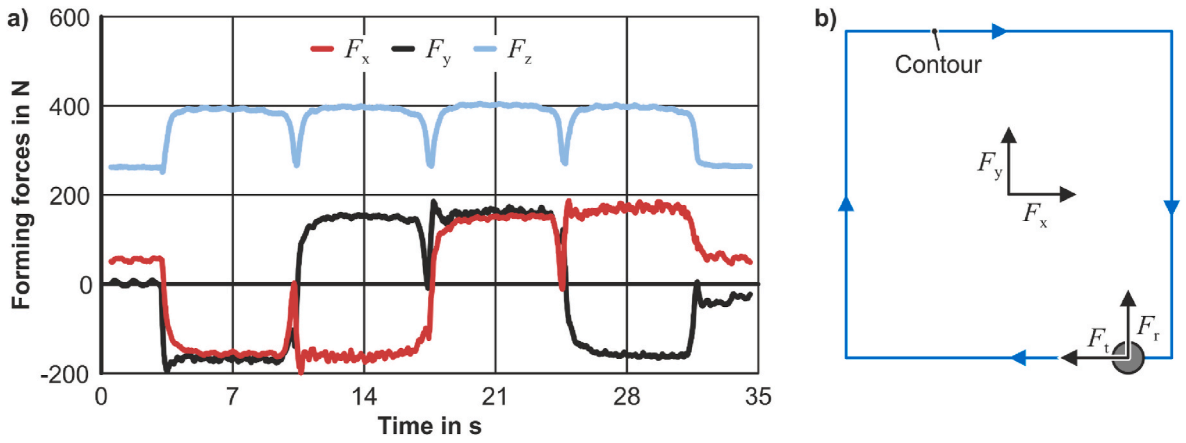

Fig. 6. (a) Signals of the continuous force measurement of the 20th contour of the convex truncated pyramid and (b) components of the forming forces in the horizontal plane.

of F_x and F_y.

The method described by Aerens et al. (2010) for calculating the horizontal forming forces for a circular tool movement was adopted for IFAM. The principle is shown for a quarter of a circle in Fig. 7a). The resulting force in the horizontal plane F_{xy}, Eq. (4), and the angle β between the measured force components F_x and F_y, Eq. (5), must first be calculated.

$$F_{xy} = \sqrt{F_x^2 + F_y^2} \tag{4}$$

$$\beta = \arctan\left(\frac{F_x}{F_y}\right) \tag{5}$$

According to Fig. 7b), the angle γ of the triangle representing the position of the tool is determined by Eq. (6).

$$\gamma = \arctan\left(\frac{y}{x}\right) \tag{6}$$

Subsequently, the orientation of F_r and F_t in relation to the resulting force F_{xy} is expressed by the angle δ, Eq. (7).

$$\delta = \frac{\pi}{2} - \beta - \gamma \tag{7}$$

Fig. 7c) depicts the last step in the calculation. The tangential forming force F_t and the radial forming force F_r are calculated by Eq. (8) and Eq. (9) respectively.

$$F_t = F_{xy} \bullet \sin\delta \tag{8}$$

$$F_r = \sqrt{F_{xy}^2 - F_t^2} \tag{9}$$

3.4. Results of the force measurement

The force and pressure trends during the convex manufacturing process in IFAM are analyzed based on a truncated pyramid, a truncated cone and an irregular shaped part as combination of both. Regarding the truncated pyramid in Fig. 8, an initial phase in the vertical force F_z followed by a steady state with approx. $F_z = 390$ N can be observed. This behavior is similar to SPIF as reported by Duflou et al. (2007). Nevertheless, there is a difference to SPIF in the fact that the force does not begin at zero since the pressure load of the active medium directly affects the tool. The tangential force reaches a maximum of $F_t = 160$ N and slowly decreases to $F_t = 145$ N at the end. The radial force F_r is almost zero at the beginning, increases significantly in the initial phase and remains nearly constant afterwards. A high pressure p is required to start the forming process, while it needs to be reduced once the first section of the part wall emerges. However, as the tool moves further to the margin, where there is interaction with the clamping of the workpiece, the pressure has to increase again to keep $\Delta h_a(i)$ close to the target value.

The force trends for shaping a truncated cone are quite similar to shaping a truncated pyramid, Fig. 9. Since the height difference $\Delta h_a(i)$ is lower than the target $\Delta h_t(i)$ in the initial phase of the forming process, the pressure p has to be increased. The distance between the circular toolpath and the rectangular clamping is larger than in the case of a rectangular toolpath resulting in less interaction at the end of the process. Therefore, the pressure does not have to rise again. Occasional outliers occur, but do not affect the overall trend.

The toolpath of the irregular-shaped part is separated into four different sections $j = \{1, 2, 3, 4\}$, Fig. 10. With a constant pressure during one contour, the force trends of each section deviate severely from each

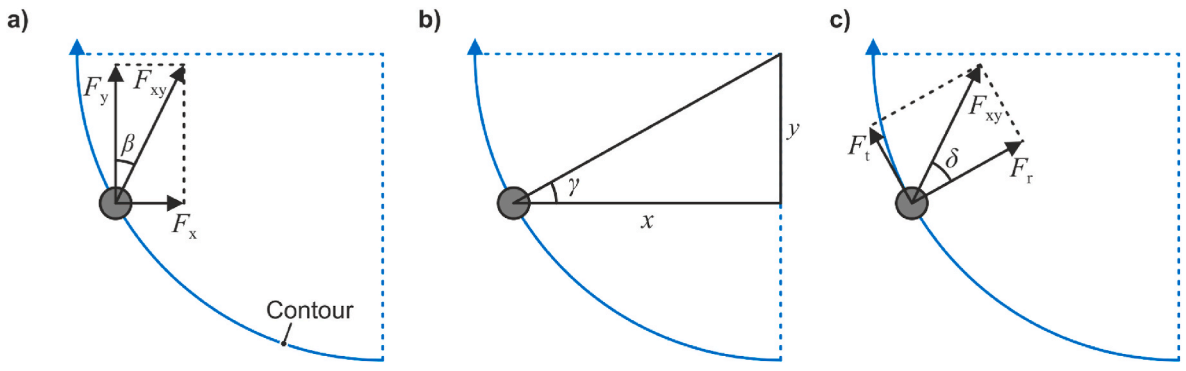

Fig. 7. (a) Forces measured in the horizontal plane, (b) position of the tool and (c) calculation of the forces in relation to the tool movement based on a quarter of the circular section.

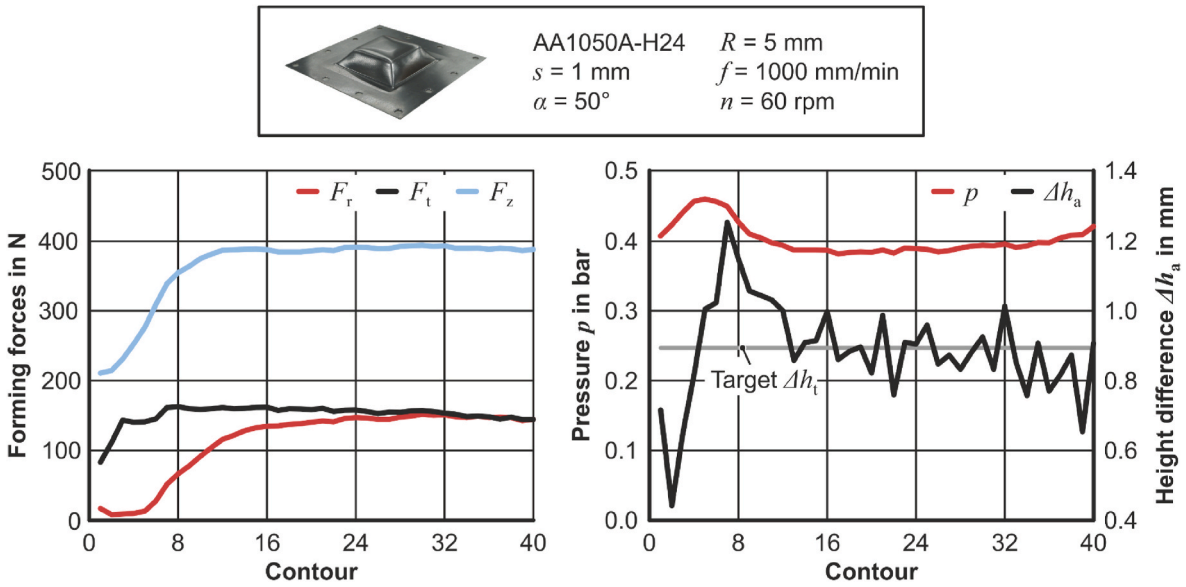

Fig. 8. Pressure and force trends of manufacturing the convex truncated pyramid.

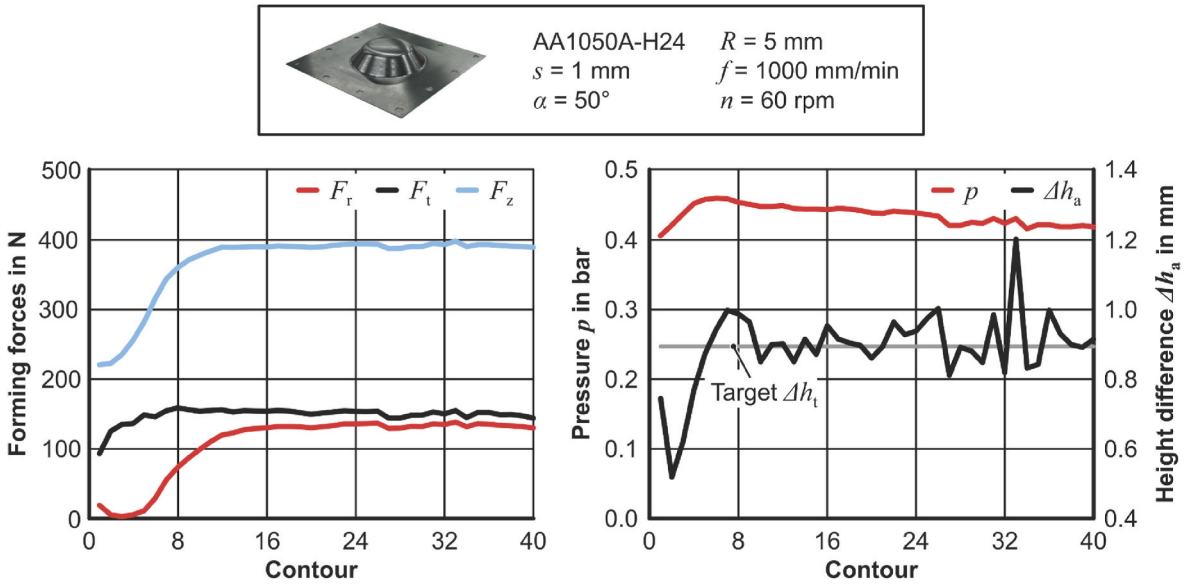

Fig. 9. Pressure and force trends of manufacturing the convex truncated cone.

other. The results show that both the vertical forming force F_z and the radial forming force F_r of the curved section ($j = 2$) are much higher than those of the other sections and rapidly decline towards the end of the manufacturing process in the flat section ($j = 4$). Moreover, the tangential force F_t of the curved section ($j = 2$) is higher than the tangential force of the corresponding truncated cone, see Fig. 9. The tangential force F_t of the flat section ($j = 4$) is lower than the reference part in Fig. 8. In summary, the force trends demonstrate that irregular shapes exhibit an inhomogeneous response towards the pressure.

The experiment reveals that the semicircular section ($j = 2$) of the irregular-shaped part emerges remarkably faster than the flat face ($j = 4$), which can be explained by the deviation of the forming forces. The top of the final workpiece has a slope along the y-axis resulting in an impaired geometrical accuracy, Fig. 11. The experiment underlines that for irregular geometries with flat and curved surfaces, the forming forces cannot be controlled using a constant pressure during one contour. It is not sufficient to use the part height after a completed contour as a control variable since it can lead to inhomogeneaus bulging and tilting of the workpiece.

The manufacturing of irregular shapes requires a control of the forming forces based on adjustment of the pressure within one contour. In the following, the correlation between the forming forces and the geometry are analyzed and modelled. The forming force components are compared to determine which has the clearest correlation to the geometry of the workpiece. Consequently, a control concept for adjusting this force is developed and tested experimentally to evaluate the improvement in the geometrical accuracy.

4. Prediction of forming forces

4.1. Experimental design

Eight convex parts were experimentally manufactured, of which four are truncated cones and four are truncated pyramids. Each part entails 40 contours with varying widths and wall angles, whereby the initial phase of the operation, represented by the first 15 contours, is not

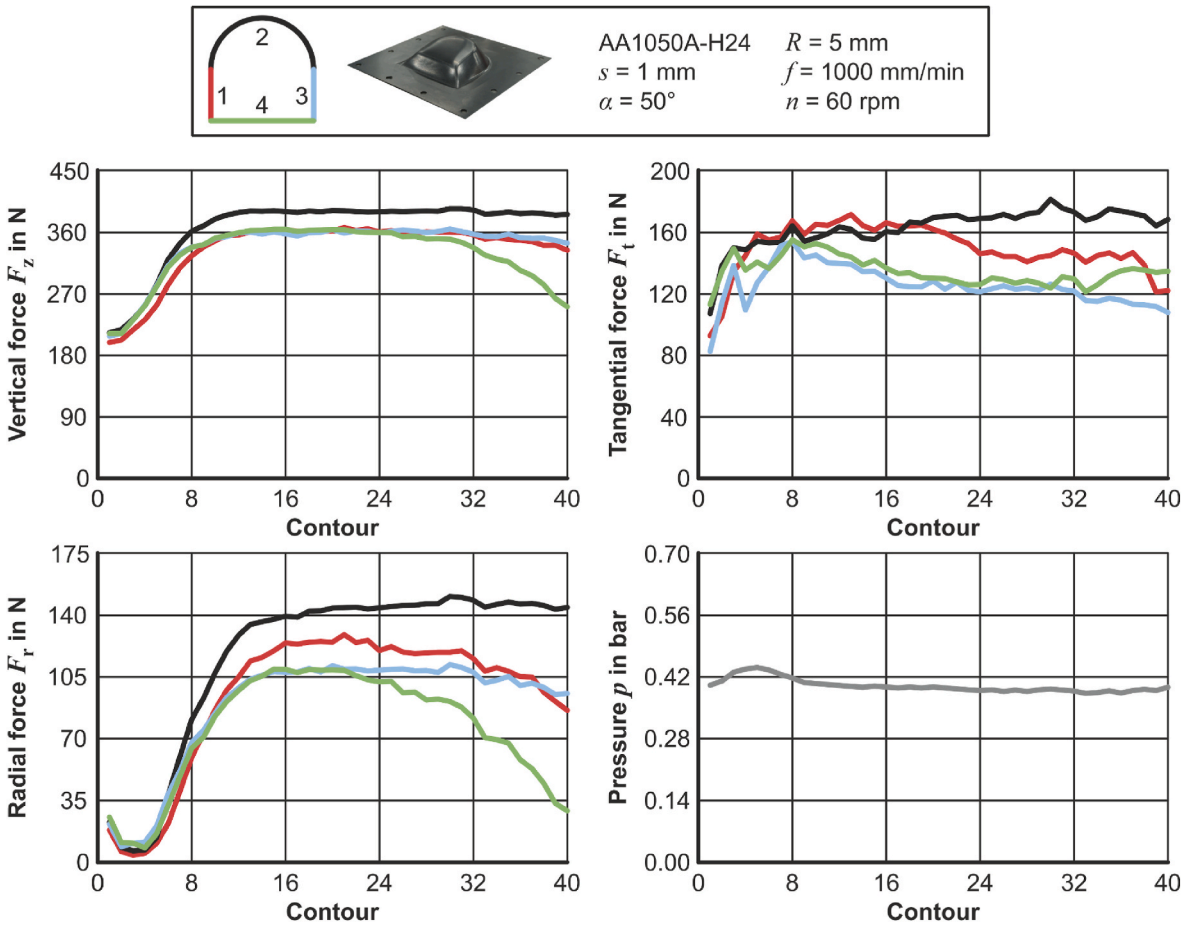

Fig. 10. Pressure and force trends of the irregular part manufactured by height control.

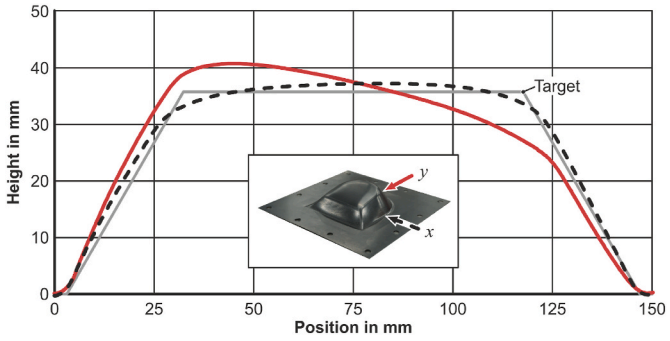

Fig. 11. Cross sections of the irregular shape manufactured by height difference control.

considered for modelling the force. The control concept, which is described in section 5.1, aims directly at the steady state. The initial phase develops automatically due to the process and does not require any targeted intervention. Thus, 25 contours for eight experiments are considered, resulting in 200 datapoints. Table 1 depicts the forming parameters for the experimental design.

4.2. Data analysis

The dataset is analyzed for correlations or associations between the predictors and the target variable. The data is continuous with the exception of the geometry variable being categorical. Bivariate analysis entails plotting two variables against each other to check for linearity and trends. It can be seen from the plots in Fig. 12 that all three of the tangential, vertical and radial forces are strongly positively correlated with the geometrical accuracy of the formed parts. The tangential force F_t in particular has a strong linear association with the height gain, making it a suitable predictor for better achieving a target geometry. It

Table 1
Experimental design for truncated pyramids and cones.

Test No.	Geometry	No. Contours	Width [mm]	R [mm]	f [mm/min]	n [rpm]	α [°]	Δh [mm]	Δx [mm]
1	Pyramid	40	{90–148.5}	5	1000	60	45	0.75	0.75
2	Pyramid	40	{90–148.5}	5	1000	60	50	0.89	0.75
3	Pyramid	40	{90–148.5}	5	1000	60	55	1.07	0.75
4	Pyramid	40	{90–148.5}	5	1000	60	60	1.29	0.75
5	Cone	40	{90–148.5}	5	1000	60	45	0.75	0.75
6	Cone	40	{90–148.5}	5	1000	60	50	0.89	0.75
7	Cone	40	{90–148.5}	5	1000	60	55	1.07	0.75
8	Cone	40	{90–148.5}	5	1000	60	60	1.29	0.75

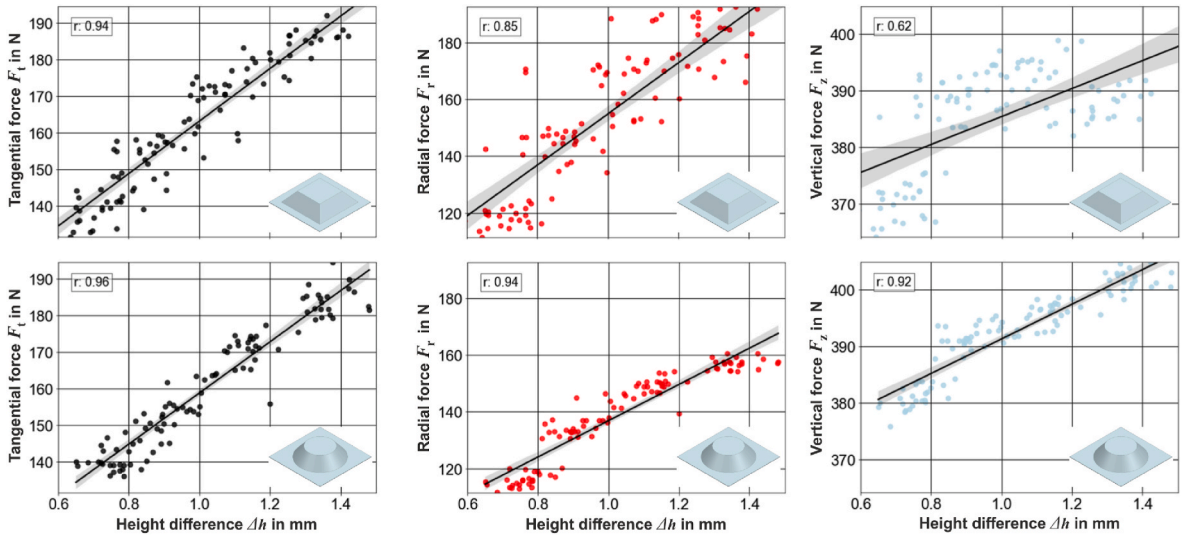

Fig. 12. The relationship between process forces in terms of height gain, from left to right: tangential, radial and vertical force for truncated pyramid (first row) and truncated cone geometries (second row).

exhibits a Pearson correlation coefficient of $r = 0.95$, where:

$$r = \frac{Cov(x_i, y_i)}{s_x s_y} = \frac{\sum_{i=1}^{n}(x_i - \bar{x})(y_i - \bar{y})}{\sqrt{\sum_{i=1}^{n}(x_i - \bar{x})^2} \cdot \sqrt{\sum_{i=1}^{n}(y_i - \bar{y})^2}}$$

with the x_i and y_i terms representing the values of x-variables and y-variables in the sample, respectively, and the $\bar{x}$ and $\bar{y}$ terms representing their mean (Sarstedt and Mooi, 2019).

The vertical forming force F_z is larger than the other force components but shows the smallest change over the height difference, Fig. 12. In addition, the Pearson correlation coefficient of r = 0.62 indicates that a linear function is not a good approximation to describe the vertical forming force F_z for truncated pyramids. Moreover, the radial force F_r has a scattered distribution of the datapoints for truncated pyramids with r = 0.85. In contrast, the tangential forming force F_t has the best linearity for both geometries. As the goal was to find a model that could adequately describe both geometries, the tangential forming force F_t was chosen as the output of the model and to be controlled in the manufacturing process. Controlling the vertical or radial forming force is possible but would require individual models for each geometry.

The data does not exhibit significant non-linearity, rendering a linear regressor sufficient for modelling. Additionally, the linear model is interpretable and reduces the risk of overfitting and limited generalization often associated with the use of more complex non-linear models on small experimental datasets. Accounting for multicollinearity, redundant independent variables were identified and eliminated, and the remaining variables of the height difference between contours Δh, the width of the contour d and the target geometry G were used to model the tangential force.

4.3. Regression model

The parameters of the model were optimized by minimizing the sum of squared errors between the actual and the predicted values of the tangential forming force F_t. The fitted linear model, shown in Fig. 13, displays a minor pattern in terms of the residuals, i.e. the difference between the observed and the predicted datapoints. For lower values of the tangential force and wall angle, it generally delivers an underestimate of the value, whereas it overestimates the values for higher values. Further, a few outliers seem to be present as well. In terms of the metrics, the model delivers an R^2 value of 0.91 and a mean absolute error of 4.1, meaning the model's estimates are, on average, 4.1 N different from the actual values. Prior to the manufacturing process, the information

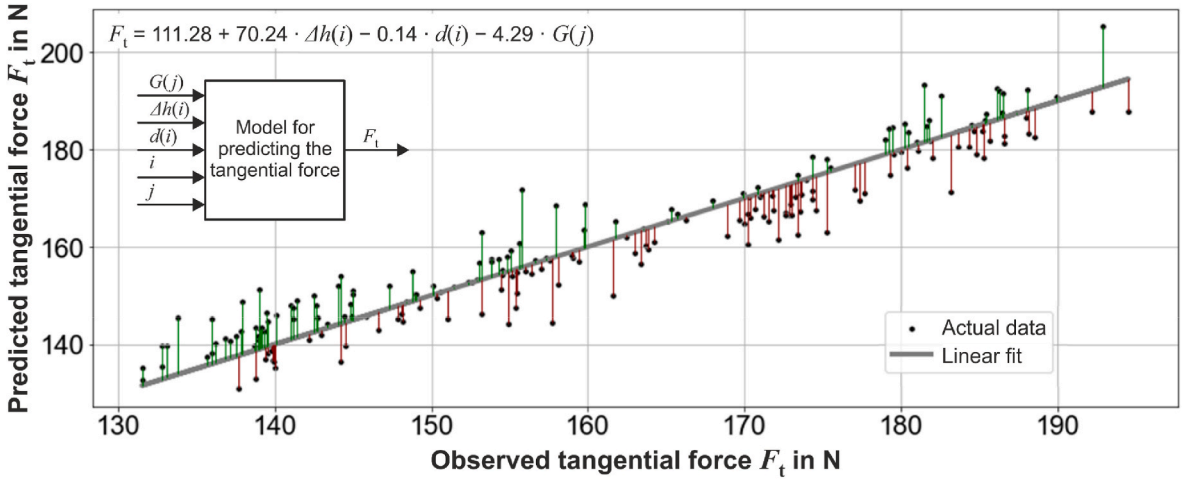

Fig. 13. Residual plot of the linear regression model predicting the tangential force based on height difference, contour width, and part geometry.

regarding the target geometry of the irregular shape is saved in a tabular format including the geometry of section $G(j)$, the desired height difference after the contour $\Delta h(i)$ and the width of the contour $d(i)$. The geometry of section $G(j)$ is encoded as a binary variable with *0* for straight sections and *1* for curved sections. The width of the contour $d(i)$ is taken from the toolpath according to Fig. 4 and Table 1. In combination with the current contour i and the section j, the model can predict the tangential force F_t needed for the force control.

5. Control of forming forces

5.1. Control concept

The aim of the discrete control concept is to ensure a specific forming force by adjusting the pressure for each section in one contour of the toolpath, Fig. 14. In combination with the current contour i and the section j, which are determined by the *NC block* sent by the control of the milling machine, the model can predict the tangential force $F(i, j)$ needed in the next section. The controller can distinguish between the different sections and sets the pressure $p(i, j)$ accordingly. Subsequently, the discrete actions of the controller become a time-continuous pressure $p(t)$ in the chamber of the set-up. The tangential force of the forming process is recorded by the measurement platform. The disturbances $e_p(t)$, which could be caused by uneven lubrication, are mentioned for the sake of completeness, but they play a subordinate role in the control concept. After each section, the mean value of the tangential force $F_t(i\text{-}1, j)$ is automatically calculated from the data.

The controller has an integral behavior described by Eq. (10). The parameter k determines how fast the controller reacts towards deviations from the target value. The parameter k was adjusted experimentally to improve the control behavior. In the following experiment, this parameter is set to $k = 0.0003$ bar/N in the first ten contours of the toolpath and afterwards increased to $k = 0.0012$ bar/N. The pressure of the first contour is set to $p(1) = 0.4$ bar for each section.

$$p(i,j) = p(i-1) + [F(i,j) - F_t(i-1,j)] \bullet k \tag{10}$$

5.2. Validation

The results indicate that by controlling the tangential force F_t for each section of the irregular-shaped part, the other force components are simultaneously stabilized, Fig. 15. The pressure while forming the flat surface ($j = 4$) is increased up to p = 0.64 bar and the pressure for the curved section ($j = 2$) is reduced to p = 0.26 bar. In general, the tangential forming forces F_t of the different sections are in better agreement with the target value and closer to each other than it is in the case of controlling the part height, see Fig. 10. Regarding the vertical forming force F_z, a steady state is reached with identical values for all sections except the first short section ($j = 1$) since the corresponding pressure is reduced significantly to $p = 0.11$ bar. This demonstrates that even similar sections of an irregular shape can show different behavior but can be individually treated by the controller.

The initial phase, which is characterized by an increase in the forming forces, is related to the development of the emerging wall angle and cannot be avoided by any type of control. Since a controller with integral behavior is selected, its reaction follows the control deviation and depends on the parameter k. The small value of k at the beginning prevents the pressure from rising too much in the initial phase, while a faster response of the controller is required in the steady state. However, small control deviations are observable in the steady state although the controller progressively adjusts the pressure level. It shows that the conditions in the forming process continuously change and are sufficiently but not entirely compensated by the controller. The conditions are dominated by how the pressure load is distributed through the workpiece into the forming zone and are influenced by the stiffness of the incrementally formed geometry. The stiffness of the machine and the tool deflection as reported by Moser et al. (2021) have a minor effect on the results of the forming process since the forming forces are small and constant. In addition, sheet thinning does not have a significant effect on the forming forces as the tool moves from the center of the sheet to the margin, so new material of initial thickness is deformed with each contour of the toolpath.

5.3. Geometrical accuracy

Controlling the tangential force leads to homogeneous forming across each section, Fig. 16. As a result, the top surface of the workpiece remains level and avoids inclination, leading to an improved geometrical accuracy compared to height difference control. However, some unwanted effects often cause small deviations from the target geometry in IFAM. One of which is the slight curvature of the top surface due to the pressure load. The edge at the transition between the top surface and the part wall is not clearly defined because the part wall requires several contours to emerge in the initial phase of the process. In addition, since the material flow is not restricted from above, the part wall can exceed the desired angle. These effects are inherent to the manufacturing process and cannot be entirely avoided, even with more precise control of the tangential forming force or by using another component of the forming force as the control variable. Supplementary strategies are required to enhance the geometrical accuracy of irregular shapes.

Nonetheless, cross-sectional comparisons show that controlling the force is more effective than controlling the height difference. In summary, the pressure has to be adjusted in a wide range for creating irregular shapes, emphasizing the importance of the control concept. Monitoring and controlling the forming forces are vital to manufacture irregular shapes for industrial applications. An application in the automotive industry could be a car fender as was created by Bambach et al. (2009) using ISF. In this regard, the transferability of both the control approach and the prediction model must be addressed. Since the aim of this work was to demonstrate the importance of controlling the forming

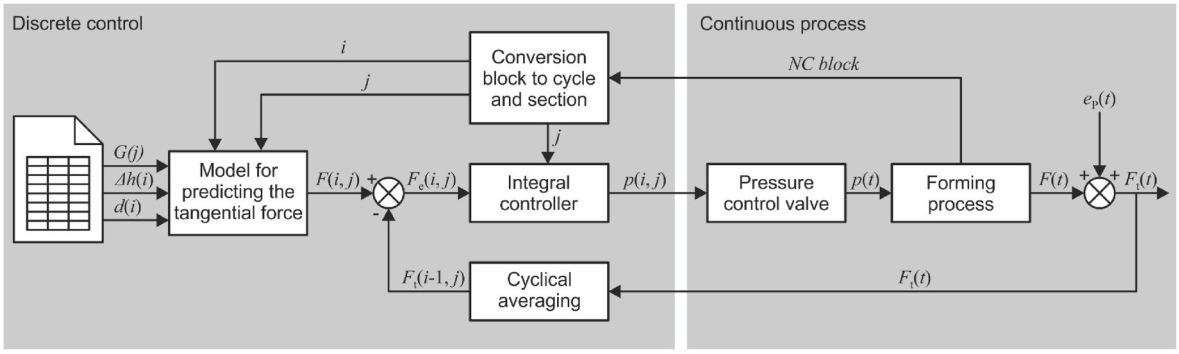

Fig. 14. Concept for controlling the tangential forming force for each section of a component.

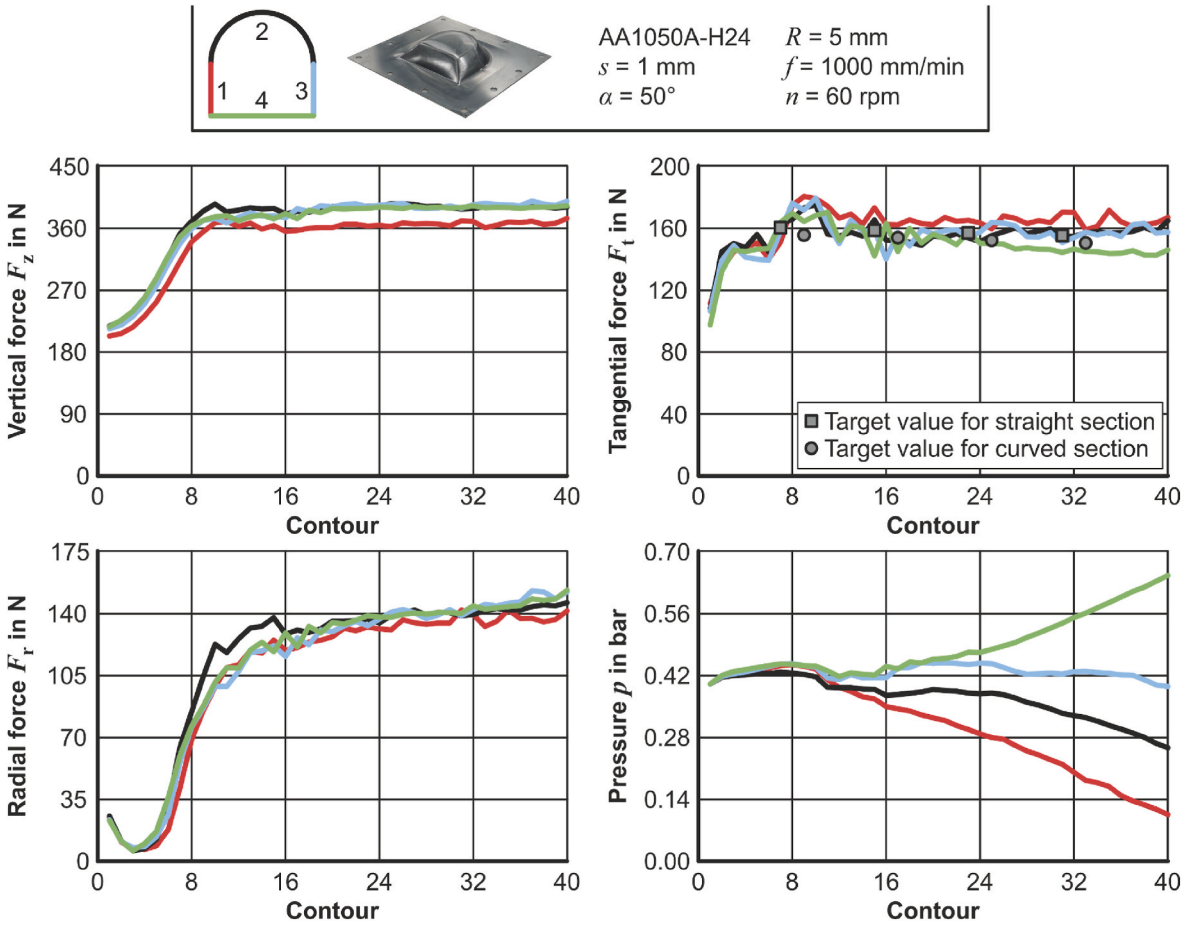

Fig. 15. Pressure and force trends of the irregular part manufactured by force control.

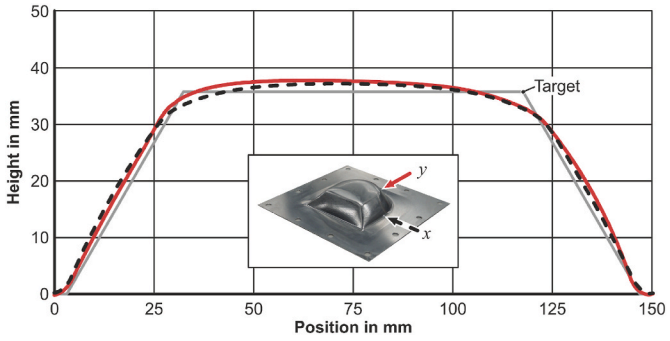

Fig. 16. Cross sections of the irregular shape manufactured by force control.

forces and to develop a general approach to create irregular shapes, the dataset was kept small, with focus on the wall angle and two types of geometries. However, the process conditions are influenced by factors such as workpiece dimensions, geometrical complexity, toolpath parameters and material properties. Variations in any of these factors will alter the forming forces and their relationship with the geometry, thereby limiting the transferability of the prediction model. In case of manufacturing a body part made of steel, a new dataset would be required to train a model for the unknown process conditions. Furthermore, the control parameter k needs to be adjusted for the best results. When manufacturing a new product, the additional time for model training and control optimization needs to be considered for the total process duration.

6. Conclusions

Truncated cones and truncated pyramids are often selected in experimental investigations for analyzing the forming mechanisms in incremental sheet forming. However, components for industrial applications are more complex and can exhibit an irregular shape. This paper explored the role of the forming forces in incremental sheet forming with active medium for manufacturing a convex irregular shape. The characteristics of the forming forces in IFAM were discussed based on a truncated cone and a truncated pyramid. A linear regression model was trained to predict the forming force in dependency of a simplified target geometry. Finally, this model was incorporated into a control concept to manufacture an irregular-shaped part with improved geometrical accuracy compared to the existing control concept that is solely focusing on the height. The following conclusion can be drawn.

1. The forming forces can be measured by integrating a table type force sensor underneath the pressure chamber. The vertical forming force has an initial phase with a rapid increase followed by a steady state. The tangential and radial forming forces also show this initial phase but can still slightly change afterwards.
2. A constant pressure is sufficient to create regular convex parts such as the truncated pyramid, which has four identical flat faces. In contrast, an irregular shape with curved and flat sections has an alternating forming behavior and cannot be homogenously shaped with a constant pressure during one contour of the toolpath.
3. By controlling the tangential forming force with the novel control concept, all components of the forming force can be stabilized for each section of the regular shape. Irregular components can be

uniformly shaped by this strategy, leading to an improved geometrical accuracy compared to controlling solely the height.

4. The results underline that the forming forces play a crucial role in a successful manufacturing process. When creating irregular shapes, the tangential forming force has a higher priority than the pressure, and the pressure must be adjusted to maintain the required forming force.

These findings provide new insights into the correlation between toolpath, pressure and forming forces in incremental sheet forming with active medium. Based on this new understanding, future work will focus on modelling more complex parameter interactions and geometrical features in order to create components with both concave and convex features.

CRediT authorship contribution statement

Sebastian Thiery: Writing – original draft, Visualization, Validation, Methodology, Data curation. **Mazhar Zein El Abdine:** Writing – original draft, Validation, Data curation. **Jens Heger:** Writing – review & editing, Supervision, Conceptualization. **Noomane Ben Khalifa:** Writing – review & editing, Supervision, Conceptualization.

Declaration of competing interest

The authors declare that they have no known competing financial interests or personal relationships that could have appeared to influence the work reported in this paper.

Acknowledgements

The authors would like to thank the German Research Foundation (DFG) for the support of the research project “manufacturing of combined convex-concave form elements by using active-medium support in incremental sheet forming” (project number: 399912095).

Data availability

The experimental data used for the linear regression are available at https://doi.org/10.25625/ZM5W4V.

References

Aerens, R., Duflou, J.R., Eyckens, P., van Bael, A., 2009. Advances in force modelling for SPIF. Int. J. Material Form. 2, 25–28. https://doi.org/10.1007/s12289-009-0536-3.

Aerens, R., Eyckens, P., van Bael, A., Duflou, J.R., 2010. Force prediction for single point incremental forming deduced from experimental and FEM observations. Int. J. Adv. Manuf. Technol. 46, 969–982. https://doi.org/10.1007/s00170-009-2160-2.

Allwood, J.M., Duncan, S.R., Cao, J., Groche, P., Hirt, G., Kinsey, B., Kuboki, T., Liewald, M., Sterzing, A., Tekkaya, A.E., 2016. Closed-loop control of product properties in metal forming. CIRP Ann. - Manuf. Technol. 65, 573–596. https://doi.org/10.1016/j.cirp.2016.06.002.

Allwood, J.M., Music, O., Raithathna, A., Duncan, S.R., 2009. Closed-loop feedback control of product properties in flexible metal forming processes with mobile tools. CIRP Ann. - Manuf. Technol. 58, 287–290. https://doi.org/10.1016/j.cirp.2009.03.065.

Bambach, M., Taleb Araghi, B., Hirt, G., 2009. Strategies to improve the geometric accuracy in asymmetric single point incremental forming. Prod. Eng. Res. Dev. 3, 145–156. https://doi.org/10.1007/s11740-009-0150-8.

Bansal, A., Lingam, R., Yadav, S.K., Venkata Reddy, N., 2017. Prediction of forming forces in single point incremental forming. J. Manuf. Process. 28, 486–493. https://doi.org/10.1016/j.jmapro.2017.04.016.

Ben Khalifa, N., Thiery, S., 2019. Incremental sheet forming with active medium. CIRP Ann. - Manuf. Technol. 68, 313–316. https://doi.org/10.1016/j.cirp.2019.04.043.

Duflou, J., Tunçkol, Y., Szekeres, A., Vanherck, P., 2007. Experimental study on force measurements for single point incremental forming. J. Mater. Process. Technol. 189, 65–72. https://doi.org/10.1016/j.jmatprotec.2007.01.005.

Duflou, J.R., Habraken, A.-M., Cao, J., Malhotra, R., Bambach, M., Adams, D., Vanhove, H., Mohammadi, A., Jeswiet, J., 2018. Single point incremental forming: state-of-the-art and prospects. Int. J. Material Form. 11, 743–773. https://doi.org/10.1007/s12289-017-1387-y.

Filice, L., Ambrogio, G., Micari, F., 2006. On-line control of single point incremental forming operations through punch force monitoring. CIRP Ann. - Manuf. Technol. 55, 245–248. https://doi.org/10.1016/S0007-8506(07)60408-9.

Fiorentino, A., 2013. Force-based failure criterion in incremental sheet forming. Int. J. Adv. Manuf. Technol. 68, 557–563. https://doi.org/10.1007/s00170-013-4777-4.

Henrard, C., Bouffioux, C., Eyckens, P., Sol, H., Duflou, J.R., van Houtte, P., van Bael, A., Duchêne, L., Habraken, A.M., 2011. Forming forces in single point incremental forming: prediction by finite element simulations, validation and sensitivity. Comput. Mech. 47, 573–590. https://doi.org/10.1007/s00466-010-0563-4.

Jeswiet, J., Duflou, J.R., Szekeres, A., 2005a. Forces in single point and two point incremental forming. AMR (Adv. Magn. Reson.) 6–8, 449–456. https://doi.org/10.4028/www.scientific.net/AMR.6-8.449.

Jeswiet, J., Micari, F., Hirt, G., Bramley, A., Duflou, J., Allwood, J., 2005b. Asymmetric single point incremental forming of sheet metal. CIRP Ann. - Manuf. Technol. 54, 88–114. https://doi.org/10.1016/S0007-8506(07)60021-3.

Li, Y., Daniel, W.J., Liu, Z., Lu, H., Meehan, P.A., 2015. Deformation mechanics and efficient force prediction in single point incremental forming. J. Mater. Process. Technol. 221, 100–111. https://doi.org/10.1016/j.jmatprotec.2015.02.009.

Li, Y., Liu, Z., Lu, H., Daniel, W.J.T., Liu, S., Meehan, P.A., 2014. Efficient force prediction for incremental sheet forming and experimental validation. Int. J. Adv. Manuf. Technol. 73, 571–587. https://doi.org/10.1007/s00170-014-5665-2.

Liu, Z., Li, Y., 2020. Small data-driven modeling of forming force in single point incremental forming using neural networks. Eng. Comput. 36, 1589–1597. https://doi.org/10.1007/s00366-019-00781-6.

Moser, N., Leem, D., Ehmann, K., Cao, J., 2021. A high-fidelity simulation of double-sided incremental forming: improving the accuracy by incorporating the effects of machine compliance. J. Mater. Process. Technol. 295. https://doi.org/10.1016/j.jmatprotec.2021.117152.

Ndip-Agbor, E., Ehmann, K., Cao, J., 2018. Automated flexible forming strategy for geometries with multiple features in double-sided incremental forming. J. Manuf. Sci. Eng. 140. https://doi.org/10.1115/1.4038511.

Ren, H., Li, F., Moser, N., Leem, D., Li, T., Ehmann, K., Cao, J., 2018. General contact force control algorithm in double-sided incremental forming. CIRP Ann. - Manuf. Technol. 67, 381–384. https://doi.org/10.1016/j.cirp.2018.04.057.

Sarstedt, M., Mooi, E., 2019. A Concise Guide to Market Research. Springer, Berlin, Heidelberg.

Taleb Araghi, B., Göttmann, A., Bambach, M., Hirt, G., Bergweiler, G., Diettrich, J., Steiners, M., Saeed-Akbari, A., 2011. Review on the development of a hybrid incremental sheet forming system for small batch sizes and individualized production. Prod. Eng. Res. Dev. 5, 393–404. https://doi.org/10.1007/s11740-011-0325-y.

Thiery, S., 2023. Grundlagenanalyse der wirkmediengestützten inkrementellen Blechumformung zur konvexen Formgebung. sierke MEDIA, Göttingen.

Thiery, S., Zein El Abdine, M., Heger, J., Ben Khalifa, N., 2021. Closed-loop control of product geometry by using an artificial neural network in incremental sheet forming with active medium. Int. J. Material Form. 14, 1319–1335. https://doi.org/10.1007/s12289-020-01598-1.

Zhu, H., Ou, H., 2023. A new analytical model for force prediction in incremental sheet forming. J. Mater. Process. Technol. 318, 118037. https://doi.org/10.1016/j.jmatprotec.2023.118037.